nature photonics

ARTICLES

https://doi.org/10.1038/s41566-019-0488-1

Efficient and stable single-layer organic light-emitting diodes based on thermally activated delayed fluorescence

Naresh B. Kotadiya, Paul W. M. Blom and Gert-Jan A. H. Wetzelaer*

From a design, optimization and fabrication perspective, an organic light-emitting diode consisting of only one single layer of a neat semiconductor would be highly attractive. Here, we demonstrate an efficient and stable organic light-emitting diode based on a single layer of a neat thermally activated delayed fluorescence emitter. By employing ohmic electron and hole contacts, charge injection is efficient and the absence of heterojunctions results in an exceptionally low operating voltage of 2.9 V at a luminance of 10,000 cd m^{-2}. Balanced electron and hole transport results in a maximum external quantum efficiency of 19% at 500 cd m^{-2} and a broadened emission zone, which greatly improves the operational stability, allowing a lifetime to 50% of the initial luminance of 1,880 h for an initial luminance of 1,000 cd m^{-2}. As a result, this single-layer concept combines high power efficiency with long lifetime in a simplified architecture, rivalling and even exceeding the performance of complex multilayer devices.

After the discovery of electroluminescence in thin films of evaporated organic small molecules[1] and conjugated polymers[2], tremendous efforts have been made to utilize these materials in electronic devices such as organic light-emitting diodes (OLEDs). Devices based on conjugated polymers were considered attractive due to their simple device structure (one organic layer sandwiched between two electrodes), opening up applications such as printable large-area flexible displays. To ensure efficient hole injection from conventional electrodes such as indium tin oxide (ITO) or poly(3,4-ethylenedioxythiophene):polystyrene sulfonate (PEDOT:PSS), the ionization energies of the organic semiconductors were designed not to be higher than ~5.3 eV. As a result, depending on the emission colour, the electron affinities then typically ranged from 2 to 3 eV. This choice in the design of organic semiconductors turned out to have a number of unfavourable consequences. First, the high electron affinity requires the use of highly reactive cathodes such as calcium or barium for efficient electron injection, putting high demands on the quality of the OLED encapsulation. Furthermore, the electron and hole transport were found to be highly unbalanced with differences up to several orders of magnitude[3]. This was found to be the result of a universal trap level situated at a depth of 3.6 eV below vacuum, leading to heavily trap-limited electron transport in organic semiconductors with low electron affinities[4]. Electron trapping confines the emission zone close to the cathode, leading to efficiency losses due to exciton quenching, as well as non-radiative trap-assisted recombination[5].

The way to overcome some of these limitations was to increase the amount of organic layers, which could easily be done using thermally evaporated molecules. In 1987, a double-layer structure consisting of a hole-transport layer and an emissive layer was used to separate the recombination zone from the electrodes[1]. In subsequent years, the efficiency of OLEDs was further improved by using more extensive multilayer structures for better tuning of the injection, charge transport and positioning of the recombination zone[6].

Another important step forward was achieved in the emissive layer by employing phosphorescent heavy-metal complexes to harvest triplet excitons[7,8], which decay non-radiatively in fluorescent emitters. These phosphorescent molecules were applied as dopants (typically 8–10 wt%) in a large-gap host to avoid concentration quenching. As a next step, it was found that the hole- and electron-transport layers can additionally be doped electrically with p- or n-type dopants, resulting in increased conductivity and, as a result, a reduced operating voltage[9–11]. The resulting p–i–n devices furthermore required the use of additional undoped exciton- and charge-blocking layers to prevent exciton quenching by the dopants, resulting typically in a five-layer device. Given that these undoped blocking layers do not necessarily consist of the same material as the host or the doped transport layers, a multilayer OLED can easily contain up to eight different organic compounds[11].

Recently, it was demonstrated that high electroluminescence quantum yields could also be obtained with metal-free organic emitters by using the concept of thermally activated delayed fluorescence (TADF)[12]. Here, the small gap between the energy of the singlet and triplet excited state allows thermally activated back transfer of the non-radiative triplet excitons to the fluorescent singlet state. Most research has been devoted to the design and fabrication of TADF OLEDs with high external quantum efficiency (EQE)[13]. However, an unresolved problem in TADF multilayer OLEDs is their limited operational stability. A notable increase in operational lifetime was achieved by using n-type hosts, resulting in a broadened recombination zone[14].

As is the case for phosphorescent OLEDs, TADF devices make use of similar complex multilayer device architectures. This complicates their design, as the properties of the charge-transport, host and blocking layers all need to be tuned to the emitter with regard to energy levels, triplet energies and charge-transport properties. The complexity further hinders interpretation of the efficiency and stability of these devices. Ideally, an OLED would consist of only one active organic semiconducting layer, in which charges are efficiently injected. Subsequently, both types of carrier are transported efficiently towards each other, after which the electrons and holes recombine through excitons with a high radiative yield via the

Max Planck Institute for Polymer Research, Mainz, Germany. *e-mail: wetzelaer@mpip-mainz.mpg.de

TADF mechanism. An advantage of TADF emitters is that they are able to harvest triplet excitons even in undoped films, so a host–guest emissive layer is not always required[15]. Balanced transport can be achieved by using an organic semiconductor with an electron affinity of ~3.6 eV (or higher) to strongly reduce or even eliminate electron trapping[4]. This would not only reduce the non-radiative recombination losses due to exciton quenching and trap-assisted recombination[5], but would also allow the use of non-reactive electron-injection layers, thereby enhancing the air stability of the device and the starting materials. A major challenge to overcome is then that a deeper lowest unoccupied molecular orbital (LUMO) of approximately −3.6 eV also leads to a lowering of the highest occupied molecular orbital (HOMO), even beyond −6 eV, to maintain the energy gap for visible light emission. Such a deep HOMO poses a significant challenge for hole injection that currently cannot be solved by p-type doped transport layers. Recently, we have developed a strategy to overcome this problem[16]. By using high-work-function transition metal oxides, such as MoO_3, in combination with an organic interlayer with a high ionization energy, ohmic hole contacts were formed on organic semiconductors with a HOMO at −6 eV and deeper. A similar strategy to create truly ohmic electron contacts would be highly desirable to enable efficient bipolar injection into an OLED device.

Here, we demonstrate that high efficiency, low operating voltage and high stability can be realized in a simplified TADF OLED comprising only a single layer of neat emitter sandwiched between ohmic electron and hole contacts. The efficient charge injection and the absence of heterojunctions lead to barrier-free flow of electrons and holes towards each other, yielding exceptionally low operating voltages. Balanced transport is achieved by choice of the energy levels of the emitter. The resulting broadened recombination zone gives rise to a greatly enhanced operational stability. Notably, the ohmic electron contact is formed without the requirement for air-sensitive dopants or injection layers, resulting in an OLED with improved air stability.

Device concept

As a candidate for the active material to be used in a single-layer OLED, we selected the TADF emitter CzDBA (9,10-bis(4-(9*H*-carbazol-9-yl)−2,6-dimethylphenyl)−9,10-diboraanthracene; Fig. 1b). This emitter has its HOMO at −5.93 and its LUMO at −3.45 eV (ref. [17]), which should be sufficiently low to alleviate the impact of electron traps on electron transport. The donor moieties of CzDBA consist of carbazole, which is a known hole-transport unit. However, the electron transport and hole transport in CzDBA have not been investigated so far. Furthermore, CzDBA showed excellent EQEs in conventional doped multilayer stack OLEDs, as well as exhibiting high photoluminescence quantum yields in both doped (~100% in 4,4′-bis(*N*-carbazolyl)−1,1′-biphenyl; CBP) and neat films (90.6%)[17].

In Fig.1a, the device layout of our single-layer OLED is shown. For hole injection, we use an interlayer of C_{60} to form an ohmic hole contact in combination with MoO_3, as we have demonstrated in earlier work[16]. For electron injection, we do not use a conventional reactive injection layer, such as LiF, calcium or barium. Instead, we use a thin (4 nm) interlayer of the electron-transport material TPBi (1,3,5-tris(*N*-phenylbenzimidazol-2-yl)benzene), which has a higher LUMO (−2.7 eV) than CzDBA, following a concept similar to the interlayer strategy for hole injection. TPBi is capped with a 100 nm Al layer, which has an effective work function of 3.4 eV at organic/evaporated metal interfaces[18].

The concept of ohmic contact formation with the help of a thin organic interlayer is based on Fermi level alignment of the electrode with the HOMO or LUMO of the active organic semiconductor. The interlayer acts as a spacer, eliminating the electrostatic interactions between electrode and organic semiconductor that result in barrier formation. The interlayer is virtually transparent for charges and thus does not result in any additional electrical resistance[16]. The interlayer can thus be regarded as part of the electrode, rather than as a charge-transport layer. As demonstrated previously for the formation of ohmic hole contacts, we now show that a similar strategy can also be applied for electron injection.

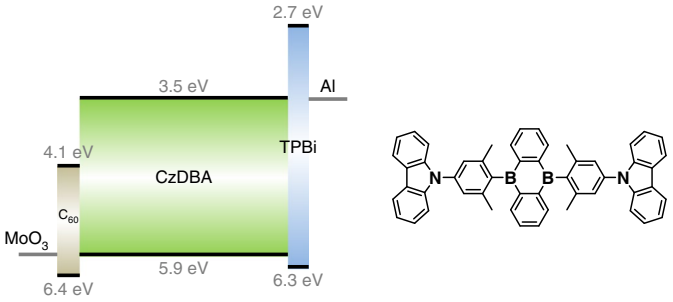

Fig. 1 | Device layout and molecular structure of the TADF emitter CzDBA. Left: schematic energy band diagram of the single-layer OLED. A CzDBA layer is sandwiched between a MoO_3 bottom anode and an Al top cathode, using a thin C_{60} and TPBi interlayer for the formation of an ohmic hole and electron contact, respectively. Right: chemical structure of CzDBA.

Results and discussion

To find out if CzDBA exhibits good charge transport, as well as to investigate electron injection from the TPBi/Al top electrode, we fabricated single-carrier devices. Electron-only devices consisted of an Al/CzDBA/TPBi(4 nm)/Al layout and hole-only devices were fabricated with a layer of CzDBA sandwiched between two ohmic C_{60}(3 nm)/MoO_3 hole contacts. The current density–voltage characteristics are displayed in Fig. 2a. The electron and hole currents are very similar, indicating balanced bipolar charge transport in CzDBA. For both electron- and hole-only devices, it is observed that the current density has a close to quadratic dependence on voltage at voltages higher than ~1 V, characteristic of a trap-free space-charge-limited current. However, at lower voltages, the current depends slightly stronger on voltage. Such behaviour corresponds to trap filling[19]. After reaching the trap-filled limit, where the voltage depends on the trap density[19], a transition to trap-free transport is observed.

To obtain quantitative charge-transport parameters, the electron and hole currents were fitted with numerical drift-diffusion simulations[20]. First, the mobility was determined at higher voltages in the trap-filled limit. The electron mobility amounted to $5\times10^{-5}\,cm^2\,V^{-1}\,s^{-1}$, whereas the hole mobility had a slightly lower value of $3\times10^{-5}\,cm^2\,V^{-1}\,s^{-1}$. Subsequently, the full J–V characteristics of the electron- and hole-only devices were fitted by including an electron-trap density of $1.4\times10^{16}\,cm^{-3}$ and a hole-trap density of $1.7\times10^{16}\,cm^{-3}$, respectively. These are remarkably low numbers of trap states, which are frequently an order of magnitude higher in organic semiconductors[4]. The obtained mobility and trapping parameters were verified for different layer thicknesses, yielding excellent agreement between simulation and experiment (see Supplementary Information). In the simulations, injection barriers were assumed to be absent. The fact that the same charge-transport parameters are obtained for different layer thicknesses shows that the newly designed TPBi/Al electrode is indeed an ohmic electron contact, notably without the use of reactive metals or n-type dopants. The obtained mobilities, although good, are not unusually high for organic semiconductors[21]. It is mainly the low trap densities for both electron and holes in combination with ohmic contacts that result in high and balanced electron and hole currents.

The balanced electron and hole mobility should also result in a broad recombination zone. This is indeed observed in the

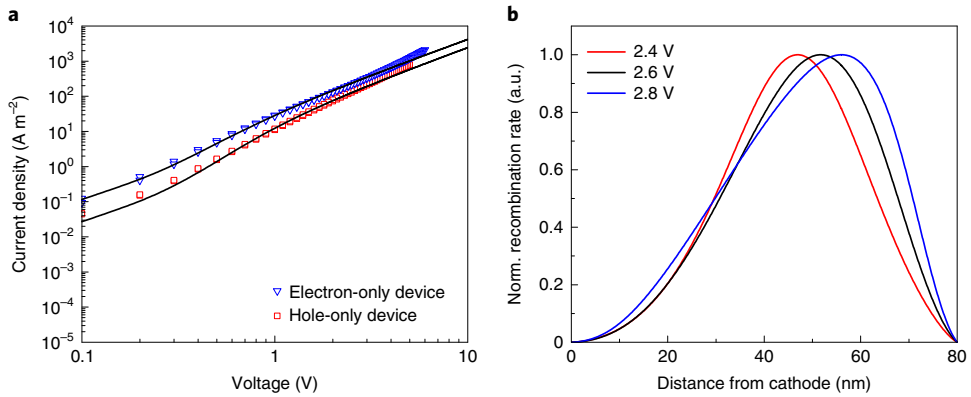

Fig. 2 | Charge transport in CzDBA and simulated recombination profile. a, Current density–voltage characteristics of CzDBA electron- and hole-only devices (symbols) with a CzDBA layer thickness of 155 nm. Solid lines are fits with a numerical drift-diffusion model. **b**, Normalized recombination profile simulated for an 80 nm CzDBA OLED at different driving voltages.

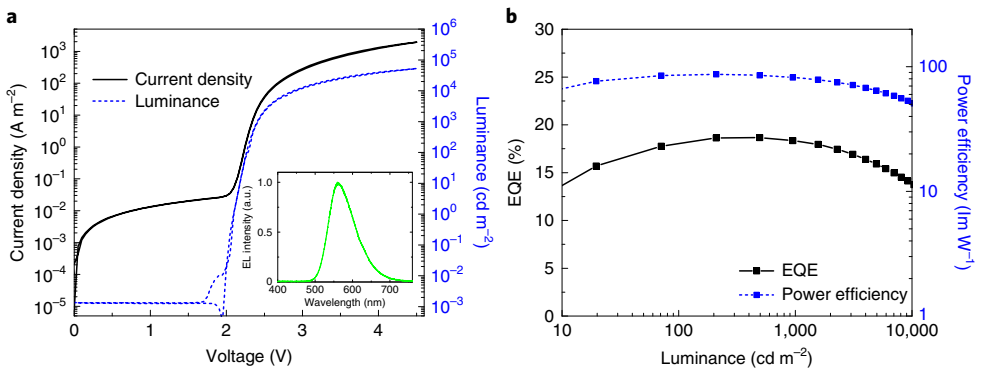

Fig. 3 | Device performance of single-layer CzDBA OLEDs. a, Current density–voltage and luminance–voltage characteristics of a CzDBA single-layer OLED with a CzDBA thickness of 75 nm. Inset: the electroluminescence (EL) spectrum, with its maximum at a wavelength of 560 nm. **b**, Corresponding EQE and power efficiency as a function of luminance.

recombination profile simulated for the CzDBA OLED (Fig. 2b). The bimolecular recombination was assumed to follow the Langevin mechanism, as is typical for single-layer OLEDs[22]. Because the electron mobility is slightly higher than the hole mobility, the recombination maximum is situated closer to the anode. The recombination zone broadens with voltage due to an increased overlap between the electron and hole density, with the maximum shifting in the anode direction. A broad recombination zone is expected to be beneficial for the operational stability of OLEDs, reducing exciton–polaron interactions associated with degradation[23–26].

Having verified nearly balanced electron and hole transport, we fabricated an OLED with the structure displayed in Fig. 1a. The measured current density and luminance as a function of voltage are shown in Fig. 3a, with the EQE displayed in Fig. 3b. The EQE reaches 19%, which is high for a single-layer OLED, but not unusual for multilayer TADF OLEDs. We note that a similar EQE has been reached previously for a multilayer stack employing a neat emissive layer instead of a host–guest system[15]. However, the corresponding single-layer device in that study yielded an EQE of only ~0.1%. We anticipate that the much higher value in our case is a combination of more balanced transport in combination with improved charge injection. In the case of ohmic injecting contacts, large densities of electrons and holes are located at the cathode and anode, respectively, as shown in the Supplementary Information, which prevents the charge carriers from reaching the opposite electrode. This effectively results in a built-in charge-blocking effect. Insertion of an additional electron- and exciton-blocking layer (CBP) between the C_{60} interlayer and CzDBA indeed did not improve the EQE (see Supplementary Information), confirming that blocking layers are not required when using ohmic contacts. Furthermore, without special measures to enhance optical outcoupling, the outcoupling losses of OLEDs are estimated to be ~70–80% (ref. [27]), meaning that our device has a high internal quantum efficiency. The light distribution pattern was measured to follow that of an ideal Lambertian source (see Supplementary Information).

Remarkably, the single-layer CzDBA OLED already reaches a luminance of 1,000 cd m^{-2} at 2.41 V and 10,000 cd m^{-2} at 2.89 V. In addition, the turn-on voltage of 2.10 V, measured at 1 cd m^{-2}, is considerably lower than the optical gap of 2.48 eV reported for CzDBA[17] and lower than the photon energy of 2.21 eV at the emission maximum, which is possible due to recombination of diffused carriers injected below the built-in voltage[28,29]. These low operating voltages are even slightly superior to state-of-the-art phosphorescent OLED stacks[9,10,30,31]. In our case, the low driving voltages are obtained without dedicated hole- and electron-transport layers and without electrical doping. Owing to the relatively high hole and electron mobility of CzDBA and in particular the low trap densities, charge transport on the emitter itself is efficient. In combination with the used ohmic contacts and the absence of further barriers induced by heterojunctions, this results in exceptionally low driving voltages. In particular at high luminance, the obtained operating voltages are markedly lower than previously reported for TADF multilayer OLEDs[32,33].

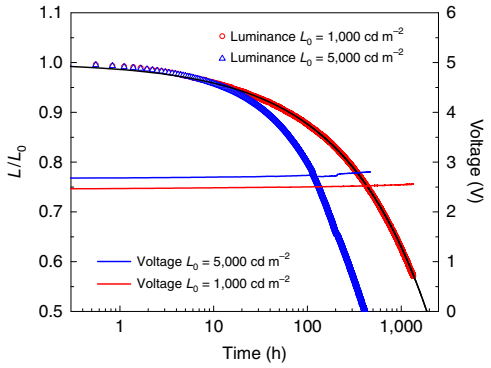

Fig. 4 | Operational lifetime of single-layer CzDBA OLEDs. Normalized luminance (symbols, left axis) and driving voltage (lines, right axis) as a function of operation time in a nitrogen atmosphere, with an initial luminance of $L_0 = 1{,}000\,\mathrm{cd\,m^{-2}}$ and $L_0 = 5{,}000\,\mathrm{cd\,m^{-2}}$ at constant driving current. The luminance decay was fitted (black line) with a function $L/L_0 = 1 - At^{(1/\alpha)}$ with $\alpha = 2.1$ (ref. [40]) to extrapolate to LT_{50} for $L_0 = 1{,}000\,\mathrm{cd\,m^{-2}}$.

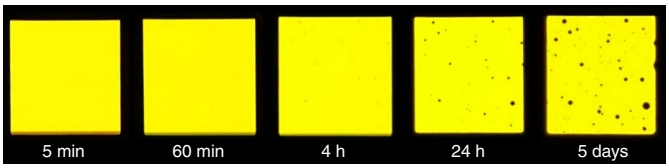

Fig. 5 | Ambient stability of a single-layer CzDBA OLED. a, Photographs of an unencapsulated CzDBA OLED operating in ambient conditions as a function of time while stored in air. The OLED has an active area of $1 \times 1\,\mathrm{cm^2}$.

The low operating voltage also results in a high power efficiency of $82\,\mathrm{lm\,W^{-1}}$ at $1{,}000\,\mathrm{cd\,m^{-2}}$, with a maximum of $87\,\mathrm{lm\,W^{-1}}$ (Fig. 3b). Power efficiencies in excess of $100\,\mathrm{lm\,W^{-1}}$ at $1{,}000\,\mathrm{cd\,m^{-2}}$ have been reported for multilayer TADF OLEDs due to a higher EQE[17,32]. However, it is important to note that the operational stability of these highly efficient TADF devices has not been reported, and extended lifetimes are usually obtained at the expense of device efficiency. As we will demonstrate below, our single-layer OLED combines high power efficiency with long lifetime.

As shown in Fig. 2b, a fairly broad emission zone is expected due to balanced bipolar transport and the absence of blocking layers. Previous research has shown that broadening of the emission zone results in increased operational stability[24,25] due to a decrease in exciton–polaron interactions[23–26]. We have performed lifetime measurements on our single-layer CzDBA OLEDs in a nitrogen atmosphere at constant current density, with initial luminance of $1{,}000\,\mathrm{cd\,m^{-2}}$ and $5{,}000\,\mathrm{cd\,m^{-2}}$. As demonstrated in Fig. 4, lifetimes to 50% of the initial luminance (LT_{50}) of 1,880 and 414 h are obtained, respectively. Interestingly, these lifetimes are markedly longer than the lifetime reported for the same CzDBA emitter in a more complex multilayer configuration. For the multilayer structure used in the degradation test in ref. [17], which has a similar power efficiency to our device at $1{,}000\,\mathrm{cd\,m^{-2}}$, the LT_{50} at $1{,}000\,\mathrm{cd\,m^{-2}}$ reached only 97 h (ref. [17]). This demonstrates that a single-layer OLED configuration can not only match the stability of a multilayer stack, but can even greatly extend the lifetime, retaining similar power efficiencies. The operational lifetimes at $5{,}000\,\mathrm{cd\,m^{-2}}$ are comparable to those obtained for the stable green TADF emitter 4CzIPN (1,2,3,4-tetrakis(carbazol-9-yl)−5,6-dicyanobenzene) in multilayer structures with n-type hosts, with similar EQE but lower operating voltage in our case, resulting in an approximately doubled power efficiency at $1{,}000\,\mathrm{cd\,m^{-2}}$ (ref. [14]). It should be noted that there is a slight difference in the emitted wavelength. In addition, the driving voltages were observed to be very stable, increasing only marginally to 2.56 V after 1,350 h of aging at $1{,}000\,\mathrm{cd\,m^{-2}}$ and to 2.80 V after reaching LT_{50} at $5{,}000\,\mathrm{cd\,m^{-2}}$ (Fig. 4), In addition, the electroluminescence spectrum was unaltered after stressing (see Supplementary Information). Besides the high operational stability, these single-layer architectures would greatly simplify a quantitative study of the cause of degradation in small-molecule OLEDs, which is a subject of further study.

These measurements show that single-layer OLEDs can be a viable or even superior alternative to multilayer stacks in terms of efficiency and operational stability. Another noteworthy feature of our OLED is the absence of reactive electron-injection layers or n-type doping. These layers are the most prominent cause of the rapid degradation of OLEDs in ambient atmosphere[34,35]. Therefore, we expect our OLED to be more stable in air. In Fig. 5, photographs are presented of an unencapsulated device operating in ambient conditions after being stored in air for set periods of time. The photographs are captured with the OLED biased at 2.15 V, corresponding to an initial luminance of ~$4\,\mathrm{cd\,m^{-2}}$. A low luminance was used to minimize flare in the photographs, aiding the visibility of the appearance of black spots. After storage in air for 4 h, the emission remains practically uniform. After 24 h of storage in air, black spots have appeared. These black spots are usually associated with oxidation or delamination of the cathode[34–36]. The black spots are still comparatively small, considering that complete device failure after a day of storage in air has been reported for some OLEDs[36,37]. After 5 days of storage in air, the black spots have grown in size, although 95% of the area still emits light. The ambient stability in air for various hours without encapsulation helps to provide flexibility in the OLED production process. An alternative example of a single-layer device with air-stable electrodes is the light-emitting electrochemical cell; however, such devices typically suffer from low operational stability and high operating voltages[38].

As a design rule for efficient OLEDs with low operating voltages, our study shows that it is more important to create ohmic contacts and use materials with a low trap density than focus on charge-carrier mobility. Although a high mobility remains important to obtain high currents at low voltages, the current is far more sensitive to injection and trapping; the latter phenomenon has received surprisingly little attention in the design of charge-transport materials and OLED stacks. Here, we have demonstrated that it is even possible to combine excellent bipolar charge-transport properties and emitter characteristics in a single organic semiconductor, providing a concept for stable and efficient single-layer OLEDs. These emitter requirements, shown here for a yellow emitter, are identical for blue- or red-emitting devices, with high photoluminescence quantum yields having been reported for many TADF emitters in neat films[39]. Furthermore, the crucial formation of ohmic contacts has been demonstrated for a wide energy range, even enabling near-ultraviolet emission with direct charge injection[16]. For the widely used green TADF emitter 4CzIPN, the presence of ohmic contacts still ensures decent device performance in a single-layer architecture, in spite of strongly unbalanced electron and hole transport (see Supplementary Information). The combination of transport and light emission in a single material and the use of ohmic contacts obviates the need for developing host, transport and blocking layers with matching energy levels and triplet energies, which is a great challenge, especially in the design of stable blue OLEDs with low operating voltages.

Conclusion

In summary, we have demonstrated that efficient and stable OLEDs can be achieved in a structure with a single layer of a TADF emitter sandwiched between two ohmic contacts. The TADF emitter

showed excellent bipolar charge transport with low trap densities, which, in combination with truly ohmic electron and hole contacts, resulted in remarkably low operating voltages. The obtained driving voltages both at low and high luminance were lower than reported for multilayer phosphorescent and TADF OLEDs featuring dedicated electron- and hole-transport layers, or p–i–n doped structures, yielding high power efficiencies. As a result of a broadened recombination zone, the operational stability could be greatly improved in comparison with a conventional multilayer OLED structure. Furthermore, the newly designed ohmic electron contact does not feature air-sensitive interlayers or n-type doping, resulting in enhanced air stability of the TADF OLED.

Online content

Any methods, additional references, Nature Research reporting summaries, source data, statements of code and data availability and associated accession codes are available at https://doi.org/10.1038/s41566-019-0488-1.

Received: 8 February 2019; Accepted: 5 June 2019;
Published online: 08 July 2019

References

1. Tang, C. W. & Van Slyke, S. A. Organic electroluminescent diodes. *Appl. Phys. Lett.* **51**, 913–915 (1987).
2. Burroughes, J. H. et al. Light-emitting diodes based on conjugated polymers. *Nature* **347**, 539–541 (1990).
3. Blom, P. W. M., De Jong, M. J. M. & Vleggaar, J. J. M. Electron and hole transport in poly(p-phenylene vinylene) devices. *Appl. Phys. Lett.* **68**, 3308–3310 (1996).
4. Nicolai, H. T. et al. Unification of trap-limited electron transport in semiconducting polymers. *Nat. Mater.* **11**, 882–887 (2012).
5. Kuik, M., Koster, L. J. A., Dijkstra, A. G., Wetzelaer, G. A. H. & Blom, P. W. M. Non-radiative recombination losses in polymer light-emitting diodes. *Org. Electron.* **13**, 969–974 (2012).
6. Kido, J., Kimura, M. & Nagai, K. Multilayer white light-emitting organic electroluminescent device. *Science* **267**, 1332–1334 (1995).
7. Baldo, M. A. et al. Highly efficient phosphorescent emission from organic electroluminescent devices. *Nature* **395**, 151–154 (1998).
8. Adachi, C. et al. Nearly 100% internal phosphorescence efficiency in an organic light-emitting device. *J. Appl. Phys.* **90**, 5048–5051 (2001).
9. Pfeiffer, M., Forrest, S. R., Leo, K. & Thompson, M. E. Electrophosphorescent p–i–n organic light emitting devices for very high efficiency flat panel displays. *Adv. Mater.* **14**, 1633–1636 (2002).
10. He, G. et al. High-efficiency and low-voltage p–i–n electrophosphorescent organic light-emitting diodes with double-emission layers. *Appl. Phys. Lett.* **85**, 3911–3913 (2004).
11. Walzer, K., Maennig, B., Pfeiffer, M. & Leo, K. Highly efficient organic devices based on electrically doped transport layers. *Chem. Rev.* **107**, 1233–1271 (2007).
12. Uoyama, H., Goushi, K., Shizu, K., Nomura, H. & Adachi, C. Highly efficient organic light-emitting diodes from delayed fluorescence. *Nature* **492**, 234–238 (2012).
13. Liu, Y., Li, C., Ren, Z., Yan, S. & Bryce, M. R. All-organic thermally activated delayed fluorescence materials for organic light-emitting diodes. *Nat. Rev. Mater.* **3**, 18020 (2018).
14. Cui, L.-S. et al. Long-lived efficient delayed fluorescence organic light-emitting diodes using n-type hosts. *Nat. Commun.* **8**, 2250 (2017).
15. Zhang, Q. et al. Nearly 100% internal quantum efficiency in undoped electroluminescent devices employing pure organic emitters. *Adv. Mater.* **27**, 2096–2100 (2015).
16. Kotadiya, N. B. et al. Universal strategy for ohmic hole injection into organic semiconductors with high ionization energies. *Nat. Mater.* **17**, 329–334 (2018).
17. Wu, T.-L. et al. Diboron compound-based organic light-emitting diodes with high efficiency and reduced efficiency roll-off. *Nat. Photon.* **12**, 235–240 (2018).
18. Zhou, M. et al. Effective work functions for the evaporated metal/organic semiconductor contacts from in-situ diode flatband potential measurements. *Appl. Phys. Lett.* **101**, 013501 (2012).
19. Kao, K.-C. & Hwang, W. *Electrical Transport in Solids* (Pergamon Press, 1981).
20. Koster, L. J. A., Smits, E. C. P., Mihailetchi, V. D. & Blom, P. W. M. Device model for the operation of polymer/fullerene bulk heterojunction solar cells. *Phys. Rev. B* **72**, 085205 (2005).
21. Shirota, Y. & Kageya, H. *Chem. Rev.* **107**, 953–1010 (2007).
22. Kuik, M. et al. Charge transport and recombination in polymer light-emitting diodes. *Adv. Mater.* **26**, 512–531 (2014).
23. Giebink, N. C. et al. Intrinsic luminance loss in phosphorescent small-molecule organic light-emitting diodes due to bimolecular annihilation reactions. *J. Appl. Phys.* **103**, 044509 (2008).
24. Zhang, Y., Lee, J. & Forrest, S. R. Tenfold increase in the lifetime of blue phosphorescent organic light-emitting diodes. *Nat. Commun.* **5**, 5008 (2014).
25. Kim, J.-M., Lee, C.-H. & Kim, J.-J. Mobility balance in the light-emitting layer governs the polaron accumulation and operational stability of organic light-emitting diodes. *Appl. Phys. Lett.* **111**, 203301 (2017).
26. Niu, Q., Rohloff, R., Wetzelaer, G.-J. A. H., Blom, P. W. M. & Crăciun, N. I. Hole trap formation in polymer light-emitting diodes under current stress. *Nat. Mater.* **17**, 557–562 (2018).
27. Meerheim, R., Furno, M., Hofmann, S., Lüssem, B. & Leo, K. Quantification of energy loss mechanisms in organic light-emitting diodes. *Appl. Phys. Lett.* **97**, 253305 (2010).
28. De Bruyn, P., van Rest, A. H. P., Wetzelaer, G. A. H., de Leeuw, D. M. & Blom, P. W. M. Diffusion-limited current in organic metal–insulator–metal diodes. *Phys. Rev. Lett.* **111**, 186801 (2013).
29. Meerheim, R., Walzer, K., He, G., Pfeiffer, M. & Leo, K. Highly efficient organic light emitting diodes (OLED) for diplays and lighting. *Proc. SPIE* **6192**, 61920P (2006).
30. Sasabe, H. et al. Extremely low operating voltage green phosphorescent organic light-emitting devices. *Adv. Funct. Mater.* **23**, 5550–5555 (2013).
31. Zhang, D. D., Qiao, J., Zhang, D. Q. & Duan, L. Ultrahigh-efficiency green PHOLEDs with a voltage under 3 V and a power efficiency of nearly 110 lm W^{-1} at luminance of 10,000 cd m^{-2}. *Adv. Mater.* **29**, 1702847 (2017).
32. Sasabe, H. et al. Ultrahigh power efficiency thermally activated delayed fluorescent OLEDs by the strategic use of electron-transport materials. *Adv. Opt. Mater.* **6**, 1800376 (2018).
33. Seino, Y., Inomata, S., Sasabe, H., Pu, Y.-J. & Kido, J. High-performance green OLEDs using thermally activated delayed fluorescence with a power efficiency of over 100 lm W^{-1}. *Adv. Mater.* **28**, 2638–2643 (2016).
34. Schaer, M., Nuesch, F., Berner, D., Leo, W. & Zuppiroli, L. Water vapor and oxygen degradation mechanisms in organic light emitting diodes. *Adv. Funct. Mater.* **11**, 116–121 (2001).
35. Van de Weijer, P., Lu, K., de Winter, S. H. P. M., Janssen, R. R. & Akkerman, H. B. Mechanism of the operational effect of black spot growth in OLEDs. *Org. Electron.* **37**, 155–162 (2016).
36. Phatak, R., Tsui, T. Y. & Aziz, H. Dependence of dark spot growth on cathode/organic interfacial adhesion in organic light emitting devices. *J. Appl. Phys.* **111**, 054512 (2012).
37. De Bruyn, P., Moet, D. J. D. & Blom, P. W. M. All-solution processed polymer light-emitting diodes with air stable metal-oxide electrodes. *Org. Electron.* **13**, 1023–1030 (2012).
38. Tang, S. et al. Design rules for light-emitting electrochemical cells delivering bright luminance at 27.5 percent external quantum efficiency. *Nat. Commun.* **8**, 1190 (2017).
39. Godumala, M., Choi, S., Cho, M. J. & Choi, D. H. Recent breakthroughs in thermally activated delayed fluorescence organic light emitting diodes containing non-doped emitting layers. *J. Mater. Chem. C* **7**, 2172–2198 (2019).
40. Silvestre, G. C. M., Johnson, M. T., Giraldo, A. & Shannon, J. M. Light degradation and voltage drift in polymer light-emitting diodes. *Appl. Phys. Lett.* **78**, 1619–1621 (2001).

Acknowledgements

We thank C. Bauer, H.-J. Guttmann and F. Keller for technical support and Y. Ie for the synthesis of 4CzIPN. This project has received funding from the European Union Horizon 2020 research and innovation programme under grant agreement no. 646176 (EXTMOS).

Author contributions

G.-J.A.H.W. proposed the project. G.-J.A.H.W. and N.B.K. designed the experiments. N.B.K. carried out device fabrication and measurements. G.-J.A.H.W. performed simulations. G.-J.A.H.W. and P.W.M.B. supervised the project and wrote the manuscript.

Competing interests

The authors declare no competing interests.

Additional information

Supplementary information is available for this paper at https://doi.org/10.1038/s41566-019-0488-1.

Reprints and permissions information is available at www.nature.com/reprints.

Correspondence and requests for materials should be addressed to G.-J.A.H.W.

Publisher's note: Springer Nature remains neutral with regard to jurisdictional claims in published maps and institutional affiliations.

Methods

Materials. CzDBA was purchased from Luminescence Technology Corporation (in sublimed grade), and C_{60} and TPBi were purchased from Sigma-Aldrich. All materials were used as received.

Device fabrication. Hole-only devices were fabricated on glass substrates prepatterned with ITO. Substrates were thoroughly cleaned by washing with detergent solution and ultrasonication in acetone and isopropyl alcohol, followed by UV–ozone treatment. A 40 nm layer of PEDOT:PSS (CLEVIOS P VP AI 4083) layer was applied by spin coating and annealed at 140 °C for 10 min in air. The substrates were then transferred into a nitrogen-filled glove box, and were not exposed to air in the subsequent steps. Next, a 6 nm layer of MoO_3, a 3 nm C_{60} interlayer, a CzDBA layer and again a 3 nm C_{60} interlayer were all thermally evaporated at a base pressure of 4×10^{-7} to 6×10^{-7} mbar. Subsequently, a MoO_3(10 nm)/Al(100 nm) top electrode was thermally evaporated to complete the device.

For electron-only devices, 35 nm of Al was thermally evaporated on cleaned glass substrates, followed by thermal evaporation of a layer of CzDBA and a 4 nm TPBi interlayer. The device was completed by evaporation of an Al(100 nm) top electrode.

For OLEDs, the device configuration was glass/ITO/PEDOT:PSS/MoO_3/C_{60}/CzDBA/TPBi/Al, where the individual layers were fabricated using the methods described above.

Measurements. Electrical characterization was carried out under a N_2 atmosphere with a Keithley 2400 source meter and light output was recorded with a Si photodiode with NIST-traceable calibration, placed close to the OLED, following a previously described procedure[41]. The EQE and power efficiency were calculated accordingly. Electroluminescence spectra were obtained with a USB4000-UV-VIS-ES spectrometer. The angular dependence of electroluminescence was obtained with a home-built set-up based on a goniometer and a Si photodiode.

Data availability

The data that support the plots within this paper and other findings of this study are available from the corresponding author upon reasonable request.

References

41. Forrest, S. R., Bradley, D. D. C. & Thompson, M. E. Measuring the efficiency of organic light-emitting devices. *Adv. Mater.* **15**, 1043–1048 (2003).